Performance Limits for Cognitive Small Cells

Matthias Wildemeersch*, Tony Q. S. Quek*†, Alberto Rabbachin‡, Cornelis H. Slump§, and Aiping Huang¶

*Institute for Infocomm Research, A*STAR, 1 Fusionopolis Way, # 21-01 Connexis, Singapore 138632
†Singapore University of Technology and Design, 20 Dover Drive, Singapore 138682
‡Massachusetts Institute of Technology, 77 Massachusetts Avenue, Cambridge, MA 02139 USA
§Signals and Systems Group, University of Twente, Drienerlolaan 5, 7500 AE Enschede, the Netherlands
¶Institute of Information and Communication Engineering, Zhejiang University, Hangzhou, China

***Abstract*—Heterogeneous networks consisting of a macrocell tier and a small cell tier are foreseen as one of the solutions to meet the ever increasing mobile data demand. Since a massive deployment of small cell access points (SAPs) leads also to a considerable increase in energy consumption, the energy efficient design of those SAPs is crucial. Sleep mode techniques are a promising strategy to reduce the energy consumption, yet they require cognitive capabilities to detect the presence of a macrocell user. In this work, we define a fundamental limit on the interference density that allows robust user detection. Beyond this limit, which we call the interference wall, an energy efficient SAP design is impossible. In addition, we elucidate the relation between energy efficiency and sensing time using large deviations theory.**

I. Introduction

Along with the exponential growth of mobile data traffic over the last years, energy consumption has risen considerably [1]. Driven by growing environmental awareness and the increasing cost of electrical energy relative to the operation of mobile base stations (MBSs), green wireless communications has become an active field of research that tries to unite the opposing needs of growing mobile data activity and energy efficiency [2]–[4].

Conventional cellular networks based on the careful deployment of MBSs suffer from reduced signal quality for indoor and cell edge users. Furthermore, the explosive surge in mobile data traffic accelerates the need for novel cellular architectures to meet such demands [1]. The LTE-Advanced standard proposes heterogeneous networks (HetNet's) that consist of a macrocell network overlayed by small cells. In this network architecture, the macro-tier guarantees the coverage, while the overlay network is a means to offload the data traffic from the macrocell network and to satisfy the local capacity demand. Although the introduction of HetNet's is able to cope with the increase of mobile data traffic, the overall energy efficiency is severely affected by the installation of additional base stations [5], [6]. Motivated by the high traffic demand fluctuations over space, time, and frequency, sleep mode techniques are a promising strategy to overcome this problem. Specifically, energy efficient SAPs can save power by entering into sleeping mode when they are not serving any active small cell users. Different sleep mode strategies for SAPs are introduced in [7], such that the wake-up mechanism can be driven by the SAP, the core network or the user equipment (UE). The wake-up mechanism governed by the UE requires reverse beaconing and adds complexity to the UE hardware, while the network controlled wake-up mechanism assumes traffic load and user localization awareness [8], [9]. Therefore, it is attractive to investigate distributed sleep mode strategies, which do not involve an augmented UE complexity and do not require signaling nor user localization awareness. To allow a distributed decision approach, the SAP requires cognitive capabilities to sense when a macrocell user is active within the SAP coverage. Considering open access control, the SAPs sense the transmissions from a macrocell user to an MBS, and switch on the pilot transmissions when user activity is detected within the SAP coverage. Due to the simplicity of passive sensing, we assume that all SAPs perform energy detection at the expense of being sensitive to noise and interference uncertainties. The detection performance of the SAP should guarantee a high probability of detection ($\mathbb{P}_{\mathrm{d}}$) to maximize traffic offload, while ensuring a low energy consumption, which is proportional to the false alarm rate ($\mathbb{P}_{\mathrm{fa}}$).

In this work, we investigate the performance limits of cognitive SAPs due to network interference uncertainties. We formulate an energy consumption model for the cognitive SAP and characterize the relationship between the energy consumption and the detection performance. Uncertainties related to the random topology, bursty activity and fading channel effects of the aggregate network interference limit the detection robustness. We define the interference wall, beyond which the target $\mathbb{P}_{\mathrm{fa}}$ and $\mathbb{P}_{\mathrm{d}}$ can not be obtained no matter how long the channel is observed. This a fundamental limit of the detection robustness, which confines a region of interferer densities where the cognitive SAP can be used advantageously in order to reduce the network wide energy consumption. In addition, we determine how fast $\mathbb{P}_{\mathrm{fa}}$ converges to a stationary value as a function of the sensing time using techniques from large deviations theory. The obtained rate function gives insight into the relationship between the detection performance and the energy efficiency.

II. System Model

A. Network topology

We consider a cellular network model that consists of a single MBS overlayed with a network of SAPs. The SAP

978-1-4673-5939-9/13/$31.00 ©2013 IEEE

applies passive sensing by means of an energy detector (ED) for reasons of low complexity and low power consumption[1] [10]. For the ED, the presence of multiple simultaneous transmissions of different UEs in the macrocell uplink band eases the detection process, and therefore, we consider the more challenging scenario with a single UE within the coverage of a single SAP. It is well known that the ED has no capabilities to differentiate between the signal of interest (SoI) and interference or noise [10]. The measurements of the SAP under realistic conditions are corrupted by network interference, which can originate from mobile macrocell users, mobile users within the SAP coverage that are not registered with the SAP operator, or from other type of underlay communications using the same uplink band [11]. As a result, we consider the case of the interfering nodes spatially distributed according to a homogeneous Poisson point process (PPP) over the entire plane. For a homogeneous PPP, the probability that k nodes reside within a region $\mathcal{R}$ depends on the interferer density λ and on the area $A_{\mathcal{R}}$ of the region $\mathcal{R}$, and can be expressed as

$$\mathbb{P}[k \in \mathcal{R}] = \frac{(\lambda A_{\mathcal{R}})^k}{k!} e^{-\lambda A_{\mathcal{R}}}, \quad k = 0, 1, 2, ... \tag{1}$$

The spatial model consisting of a macrocell overlayed with multiple small cells is illustrated in Fig. 1.

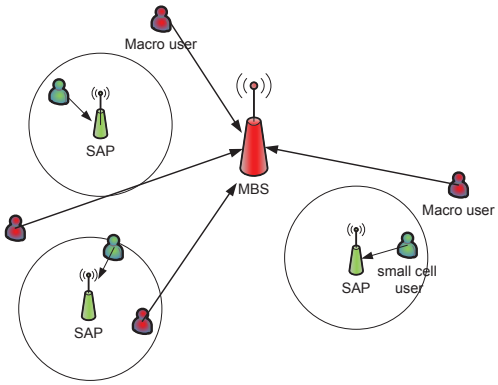

Fig. 1. Spatial distribution of the SAPs and the UEs. The interfering nodes consist of the macrocell users outside the coverage of the set of SAPs, and macrocell users within the coverage of an SAP who are not registered with the SAP operator.

B. SAP power consumption

The SAPs operate in open access (OA) mode and are accessible for all users registered with the operator of the SAP. In order to enable a distributed sleep/wake-up scheme, the SAPs are provided with cognitive capabilities. When the SAP does not serve an active user call, it goes into sleep mode and senses periodically the macrocell uplink channel to detect user activity. Once the SAP detects an active user in the macrocell uplink band within its coverage, the SAP switches on and starts the transmission of pilot signals. Subsequently, the UE reports the presence of the SAP to the MBS and the UE is handed over to the SAP. The activity of the SAP is defined using a time-slotted model. Assuming a fixed slot duration T, the SAP senses the channel over a sensing time τ_s and transmits over a time $T - \tau_s$ when an active mobile user is detected. Three main contributions to the power consumption of the cognitive SAP can be identified: the power related to the circuit synchronization Ξ_c, the sensing power Ξ_s, and the transmission power Ξ_t [12]. We consider the circuit synchronization to be active over the entire time slot. The SAP senses the uplink channel according to a sensing scheme with sensing probability $p_{\rm s}$ and the corresponding energy consumption is proportional to the sensing time. The activity of the SAP, the UE and the interfering nodes on a given instant can be modeled as mutually independent Bernouilli processes with success probabilities $p_{\rm s}$, $p_{\rm u}$ and $p_{\rm I}$, respectively. By the colouring theorem of PPPs, the active nodes that contribute to the interference form a PPP with density $p_{\rm I}\lambda$. The UE signal detection is a binary hypothesis test problem. In the presence of the UE signal (hypothesis $\mathcal{H}_1$), the SAP starts the pilot transmissions when it senses the uplink channel and correctly detects the user activity. In the absence of the UE signal (hypothesis $\mathcal{H}_0$), the SAP starts the pilot transmissions when it incorrectly detects the presence of a user. Therefore, the power consumption can be modeled as

$$\begin{aligned} E_{\rm tot} = \Xi_c T + p_{\rm u} \left\{ p_{\rm s} \left[\Xi_s \tau_s + \mathbb{P}_{\rm d} \Xi_t (T - \tau_s) \right] \right\} + \\ (1 - p_{\rm u}) \left\{ p_{\rm s} \left[\Xi_s \tau_s + \mathbb{P}_{\rm fa} \Xi_t (T - \tau_s) \right] \right\}. \end{aligned} \tag{2}$$

Note that the energy consumption is linear with respect to $\mathbb{P}_{\rm d}$ and $\mathbb{P}_{\rm fa}$.

C. Non-coherent detection performance

At the cognitive SAP, the received signal can be written as

$$\begin{aligned} \mathcal{H}_0 : r(t) &= n(t) + i(t) \\ \mathcal{H}_1 : r(t) &= \frac{h(t)}{r_{\rm f}^{\nu/2}} s(t) + n(t) + i(t) \end{aligned} \tag{3}$$

where $s(t)$, $n(t)$, and $i(t)$ represent the SoI, the additive white Gaussian noise and the aggregate network interference, respectively. The impulse response of the flat fading channel between the UE and SAP is represented by $h(t)$, $r_{\rm f}$ is the distance between the UE and the SAP, and ν is the power path loss exponent. To facilitate the analysis, we consider that the SAP is at the origin of the Euclidean plane and the coverage of the SAP is a circular area around the origin with radius R. The power of the SoI at the SAP can be written as $P_{\rm u} r_{\rm f}^{-\nu} h^2$, where $P_{\rm u}$ is the transmit power of the UE.

The decision variable V determines the presence or absence of the SoI. For the ED, V is defined as

$$V = \frac{1}{\tau_s} \int_0^{\tau_s} \left(\frac{h(t)}{r_{\rm f}^{\nu/2}} s(t) + n(t) + i(t) \right)^2 dt. \tag{4}$$

[1]Note that the ED sets a lower bound on the detection performance.

After sampling and considering block fading, the decision variable can be expressed as

$$V_{\mathrm{ED}} = \frac{1}{N}\sum_{k=1}^{N} r^2[k] = \frac{1}{N}\sum_{k=1}^{N}\left(\frac{h}{r_{\mathrm{f}}^{\nu/2}}s[k] + i[k] + n[k]\right)^2 \tag{5}$$

where $N = \lfloor \tau_s f_s \rfloor$ with f_s as the sampling frequency equal to the Nyquist rate[2]. The probability of detection is defined as the probability that V_{ED} surpasses the threshold β in the presence of the SoI and is given by $\mathbb{P}_{\mathrm{d}} = \mathbb{P}[V_{\mathrm{ED}} > \beta|\mathcal{H}_1]$. The probability of false alarm is defined as the probability that V_{ED} surpasses the threshold in absence of the SoI and is given by $\mathbb{P}_{\mathrm{fa}} = \mathbb{P}[V_{\mathrm{ED}} > \beta|\mathcal{H}_0]$. The noise term has a zero-mean Gaussian distribution $n(t) \sim \mathcal{N}(0, \sigma_{\mathrm{n}}^2)$. We assume the distance, the fading distribution and the noise variance to be known, the signal structure unknown though deterministic, and we model the interference as additive white Gaussian noise with variance σ_{i}^2. The decision variable follows a central chi-square and a non-central chi-square distribution under $\mathcal{H}_0$ and $\mathcal{H}_1$, respectively. For realistic values of the sensing time N and applying the central limit theorem, V_{ED} can be approximated by a Gaussian random variable (r.v.)

$$\begin{aligned} V_{\mathrm{ED}|\mathcal{H}_0} &\sim \mathcal{N}(\sigma_{\mathrm{tot}}^2, 2\sigma_{\mathrm{tot}}^4/N) \\ V_{\mathrm{ED}\sigma_{\mathrm{n}}^2|\mathcal{H}_1} &\sim \mathcal{N}(P_{\mathrm{u}} r_{\mathrm{f}}^{-\nu} h^2 + \sigma_{\mathrm{tot}}^2, 2(P_{\mathrm{u}} r_{\mathrm{f}}^{-\nu} h^2 + \sigma_{\mathrm{tot}}^2)^2/N) \end{aligned} \tag{6}$$

where $\sigma_{\mathrm{tot}}^2 = \sigma_{\mathrm{n}}^2 + \sigma_{\mathrm{i}}^2$. Hence, $\mathbb{P}_{\mathrm{fa}}$ and $\mathbb{P}_{\mathrm{d}}$ can be found in terms of $\mathcal{Q}$-functions and are given by [13]

$$\mathbb{P}_{\mathrm{fa}} = \mathcal{Q}\left(\frac{\beta - \sigma_{tot}^2}{\sqrt{2/N}\sigma_{\mathrm{tot}}^2}\right), \mathbb{P}_{\mathrm{d}} = \mathcal{Q}\left(\frac{\beta - (P_{\mathrm{r}} + \sigma_{tot}^2)}{\sqrt{2/N}(P_{\mathrm{r}} + \sigma_{\mathrm{tot}}^2)}\right) \tag{7}$$

where $P_{\mathrm{r}} = P_{\mathrm{u}} r_{\mathrm{f}}^{-\nu} h^2$, and where the $\mathcal{Q}$-function represents the tail probability of the normal distribution.

III. Interference wall

In [14], environment-dependent uncertainties are shown to be the cause of the so-called SNR wall, below which the detector is not robust regardless the sensing time. Noise uncertainty caused by the noise estimation has been discussed in [15]. An SAP with a UE within its coverage finds itself in a high-SNR environment, and therefore, the SNR-wall due to noise estimation is not relevant in this scenario. However, another source of uncertainty is the network interference [16]. In the following, we derive an expression of the uncertainty due to the network interference.

A. Unbounded path-loss model

The interfering nodes can be mobile users that do not have access to the SAP, or other (cognitive) devices that use the same band as the macrocell users. Therefore, the aggregate network interference measured at the SAP can be written as

$$i(t) = \mathfrak{Re}\left\{\sum_{l=1}^{\infty} i_l(t)\right\} = \mathfrak{Re}\left\{\sum_{l=1}^{\infty} \frac{h_l \mathbf{X}_l^{\mathrm{i}}}{r_{\mathrm{f},l}^{\nu/2}}\right\}, \tag{8}$$

[2]For simplicity, we assume $N = \tau_s f_s$

where we model $\mathbf{X}_l^{\mathrm{i}} = X_{l,1}^{\mathrm{i}} + jX_{l,2}^{\mathrm{i}}$ as zero-mean complex r.v.. Note that the r.v.'s $\mathbf{X}_l^{\mathrm{i}}$ are circular symmetric, and independent and identically distributed (i.i.d.) in l since the interferers transmit independently. Therefore, with the interfering nodes scattered over $\mathbb{R}^2$ according to a PPP, the aggregate network interference follows a symmetric stable distribution [17]

$$i \sim \mathcal{S}(\alpha = 4/\nu, \beta = 0, \gamma = \pi\lambda C_{4/\nu}^{-1}\mathbb{E}[|h_l X_{l,p}^{\mathrm{i}}|^{4/\nu}]) \tag{9}$$

with C_x defined as

$$C_x \triangleq \begin{cases} \frac{(1-x)}{\Gamma(2-x)\cos(\pi x/2)}, & x \neq 1, \\ \frac{2}{\pi}, & x = 1. \end{cases} \tag{10}$$

Since the network interference follows a symmetric stable distribution, the decomposition property can be applied and the interference can be represented as $i = \sqrt{U}G$, with $U \sim \mathcal{S}(2/\nu, 1, \cos(\frac{\pi}{\nu}))$ and $G \sim \mathcal{N}(0, 2\gamma^{\nu/2})$. Therefore, the received signal under $\mathcal{H}_0$ conditioned on U can be expressed as a normal r.v. $r_{k|\mathcal{H}_0,U} \sim \mathcal{N}(0, \sigma_{\mathrm{n}}^2 + 2\gamma^{\nu/2}U)$. With γ defined in (9), the variance of $r_{k|\mathcal{H}_0,U}$ can be written as $\sigma_{\mathrm{tot}}^2 = \sigma_{\mathrm{n}}^2 + 2\gamma^{\nu/2}U = \sigma_{\mathrm{n}}^2(1 + 2\eta_i(\pi C_{4/\nu}^{-1}\mathbb{E}[|h_l X_{l,p}^{\mathrm{i}}|^{4/\nu}])^{\nu/2}\lambda^{\nu/2}U)$, where η_i is the INR. Let $G = 2\eta_i(\pi C_{4/\nu}^{-1}\mathbb{E}[|h_l X_{l,p}^{\mathrm{i}}|^{4/\nu}])^{\nu/2}U)$, then the total variance takes values in the interval $\sigma_{\mathrm{tot}}^2 \in [\sigma_{\mathrm{n}}^2, \sigma_{\mathrm{n}}^2(1 + \lambda^{\nu/2}G)]$ since the skewed stable distribution U only takes positive values. To be robust with respect to the network interference, (7) is modified and we get

$$\begin{aligned} \mathbb{P}_{\mathrm{fa}} &= \mathcal{Q}\left(\frac{\beta - (1 + \lambda^{\nu/2}G)\sigma_{\mathrm{n}}^2}{\sqrt{2/N}(1 + \lambda^{\nu/2}G)\sigma_{\mathrm{n}}^2}\right) \\ \mathbb{P}_{\mathrm{d}} &= \mathcal{Q}\left(\frac{\beta - (1 + \mathrm{SNR})\sigma_{\mathrm{n}}^2}{\sqrt{2/N}(1 + \mathrm{SNR})\sigma_{\mathrm{n}}^2}\right). \end{aligned} \tag{11}$$

We define the sample complexity as the sensing time required to obtain a target $\mathbb{P}_{\mathrm{d}}$ and $\mathbb{P}_{\mathrm{fa}}$. Eliminating β from the equations in (11) and solving to N, the sample complexity can be written as

$$N = \frac{2(\mathcal{Q}^{-1}(\mathbb{P}_{\mathrm{fa}})(1 + G\lambda^2) - \mathcal{Q}^{-1}(\mathbb{P}_{\mathrm{d}})(1 + \mathrm{SNR}))^2}{(\mathrm{SNR} - G\lambda^{\nu/2})^2}. \tag{12}$$

It follows that as $\lambda \to (\mathrm{SNR}/G)^{2/\nu}$, we have $N \to \infty$. In other words, a target $\mathbb{P}_{\mathrm{fa}}$ and $\mathbb{P}_{\mathrm{d}}$ cannot be attained within a finite sensing time for some interfering node density approaching $(\mathrm{SNR}/G)^{2/\nu}$. We call this limit the interference wall $\lambda_{\mathrm{wall,s}}$ and note that $\lambda_{\mathrm{wall,s}}$ is a function of the SNR, INR, the power path loss exponent and the fading. However, to calculate G, a percentile of the distribution has to be selected that corresponds to a worst case, due to the heavy tails of the stable distribution.

B. Bounded path-loss model

The heuristic approximation based on the stable distribution is computationally intensive and sensitive to the selection of the percentile. In order to find a solution with a higher accuracy, we consider that the interferers are located in

$$\mathcal{I} = \frac{2}{\nu/2-1}(d_{\min}^{2-\nu} - d_{\max}^{2-\nu}) \left(\frac{(\alpha-3)(\alpha-2)(d_{\min}^{2-\nu} - d_{\max}^{2-\nu})(\nu-1)}{(d_{\min}^{2-2\nu} - d_{\max}^{2-2\nu})(\nu/2-1)P_{\mathrm{i}}\sigma_h^2} \right)^{\frac{2-\alpha}{2}+\frac{1}{2}(\alpha-2)} \eta_i \pi \sigma_h^2 \tag{15}$$

the annulus $\mathcal{A}$, defined by the radii $d_{\min}$ and $d_{\max}$. Under such conditions, it can be shown that the aggregate network interference follows a truncated stable distribution [18]

$$i_k \sim S_t(\gamma', \alpha = 4/\nu, g), \tag{13}$$

where α corresponds to the characteristic exponent of the stable distribution, γ' corresponds to the dispersion, and g reflects the decaying of the tail of the truncated stable distribution. The coefficients γ' and g can be determined by the method of the cumulants, by imposing the equality of the second and fourth cumulant of the truncated stable distribution with the respective cumulants of the network interference. Applying the approach of Section III-A based on (7), we further approximate the network interference by a Gaussian r.v., such that the received signal follows a normal distribution $r_{k|\mathcal{H}_0} \sim \mathcal{N}(0, \sigma_{\mathrm{n}}^2 + \sigma_{\mathrm{i}}^2)$, where σ_{i}^2 represents the second order moment of the truncated stable distribution

$$\sigma_{\mathrm{i}}^2 = \mathbb{E}[i_k^2] = \frac{\partial^2 M_{\mathrm{i}}(k,\lambda)}{\partial k^2}|_{k=0} = \sigma_{\mathrm{n}}^2 \mathcal{I}\lambda \tag{14}$$

where $M_{\mathrm{i}}(k,\lambda)$ is the moment generating function (MGF) of the truncated stable distribution. After some manipulations, $\mathcal{I}$ can be expressed as in (15) at the top of this page. Note that the variance of the network interference is linear in the interferer density λ and the parameter $\mathcal{I} = f(d_{\min}, d_{\max}, \nu, \eta_i, \sigma_h^2)$. For $\nu = 4$, the parameter $\mathcal{I}$ further simplifies to $2(d_{\min}^{-2} - d_{\max}^{-2})P_{\mathrm{i}}\pi\sigma_h^2$. Eliminating β from the expressions of $\mathbb{P}_{\mathrm{d}}$ and $\mathbb{P}_{\mathrm{fa}}$, the sample complexity can now be expressed as

$$N = \frac{2(\mathcal{Q}^{-1}(\mathbb{P}_{\mathrm{fa}})(1+\mathcal{I}\lambda) - \mathcal{Q}^{-1}(\mathbb{P}_{\mathrm{d}})(1+\mathrm{SNR}))^2}{(\mathrm{SNR} - \mathcal{I}\lambda)^2} \tag{16}$$

and the interference wall is given by $\lambda_{\mathrm{wall,t}} = \mathrm{SNR}/\mathcal{I}$.

IV. False alarm decay

In this section, we determine how fast $\mathbb{P}_{\mathrm{fa}}$ converges to its target value, to express the relationship between energy efficiency and interfering node density. From (2), we notice that the energy consumption is linear in $\mathbb{P}_{\mathrm{d}}$ and $\mathbb{P}_{\mathrm{fa}}$. A direct method to obtain the PDF of V_{ED} as a function of the sensing time is cumbersome. Instead, we will use tools from large deviations theory to determine how fast the target $\mathbb{P}_{\mathrm{fa}}$ can be reached. According to the Cramer theorem, we have for interference-limited networks

$$\mathbb{P}_{\mathrm{fa}}(\beta) = \mathbb{P}[1/N \sum_{N} i_k^2 > \beta] \leq e^{-NI(\beta)} \tag{17}$$

which decays exponentially with the sensing time and the decay rate is determined by the rate function $I(x)$. In order to have finite moments, we model the aggregate interference power i_k^2 according to a truncated stable distribution. The CF of the truncated stable distribution is given by [19]

$$\psi_{i_k^2}(j\omega) = \exp\left(\gamma'\Gamma(\alpha')\left[(g-j\omega)^{\alpha'} - g^{\alpha'}\right]\right) \tag{18}$$

where α' is chosen equal to the characteristic exponent of the stable distribution in the unbounded path loss model. The parameters of the truncated stable distribution can be found using the method of the cumulants. From (18), the cumulants of the truncated stable distribution can be expressed as

$$\begin{aligned} \kappa_I(n) &= \frac{1}{j^n}\frac{d^n}{d\omega^n} \ln \psi_{i_k^2}(j\omega)\Big|_{\omega=0} \\ &= (-1)^n \gamma' \Gamma(-\alpha') g^{\alpha'-n} \Pi_{i=0}^{n-1}(\alpha'-i). \end{aligned} \tag{19}$$

Building on Cambell's theorem [18], the cumulants of the aggregate interference can be expressed as

$$\kappa(n) = P_{\mathrm{i}}^n \frac{\pi\lambda}{1-n\nu}(d_{\max}^{2-2n\nu} - d_{\min}^{2-2n\nu})\mu_{h^2}(n). \tag{20}$$

Using (19) and (20), the parameters γ' and g can be written as a function of the first two cumulants as follows

$$\begin{aligned} \gamma' &= \frac{-\kappa(1)}{\Gamma(-\alpha')\alpha'\left(\frac{\kappa(1)(1-\alpha')}{\kappa(2)}\right)^{\alpha'-1}} \\ g &= \frac{\kappa(1)(1-\alpha')}{\kappa(2)}. \end{aligned} \tag{21}$$

Since i_k^2 are assumed to be i.i.d., the Cramer theorem can be applied and we can express the rate function as the Legendre-Fenchel transform of the logarithmic MGF

$$I(x) = \sup_{\theta}\left(\theta x - \gamma'\Gamma(-\alpha')[(g-\theta)^{\alpha'} - g^{\alpha'}]\right). \tag{22}$$

For $\theta < g$, let the first derivative be equal to zero and solving to θ for $\nu = 4$, we have

$$\theta = g - \left(\frac{-\gamma'\Gamma(-\alpha')}{2x}\right)^2. \tag{23}$$

Substituting θ in (22), the expression of the rate function is given by

$$I(x) = gx + \sqrt{g}\gamma'\Gamma(-\alpha) + \frac{(\gamma'\Gamma(-\alpha'))^2}{4x}. \tag{24}$$

V. Numerical Results

Figure 2 shows the sample complexity to satisfy a target $\mathbb{P}_{\mathrm{fa}}$ and $\mathbb{P}_{\mathrm{d}}$ for increasing interferer density. This figure illustrates the fundamental limit of the interfering node density under which the SAP can robustly detect the macrocell user presence. Beyond the interference wall, the noise uncertainty becomes too big to distinguish between SoI or noise. The curves are drawn using the 87 percentile of the stable distribution, the truncated stable distribution and numerical

simulations. We consider SNR = 3 dB defined for the UE at the edge of the SAP coverage $R = 20$, while INR = 20 dB defined at a distance of 1 meter (far-field assumption). For $d_{\min} = 1$ and $d_{\max} = 100$, the approaches with the stable and the truncated stable distribution are in good agreement and correspond also quite well with the numerical simulation. The decay rate of $\mathbb{P}_{\text{fa}}$ is expressed in (24) and reflects the

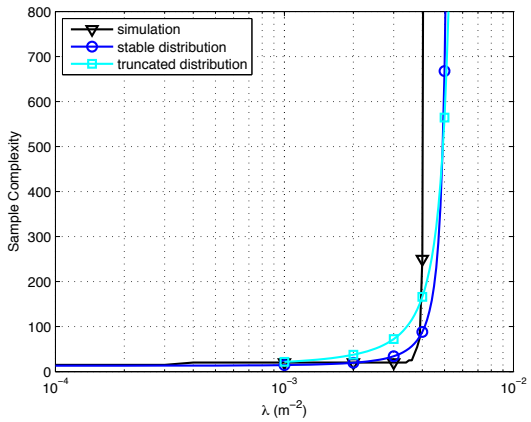

Fig. 2. The interference wall using the approximation with the 87 percentile of the stable distribution, using the truncated stable distribution and using numerical simulations for $\mathbb{P}_{\text{fa}} = 0.1$ and $\mathbb{P}_{\text{d}} = 0.9$, SNR = 3 dB, INR = 20 dB, and $\nu = 4$.

achievable energy efficiency. Figure 3 shows the decay rate as a function of the threshold x for different values of the interference power and the interferer density. It can be observed that with increasing density and interference power the rate function decreases. Thus, the rate function can reveal more insight into the effect of λ and P_{i} on the SAP power consumption.

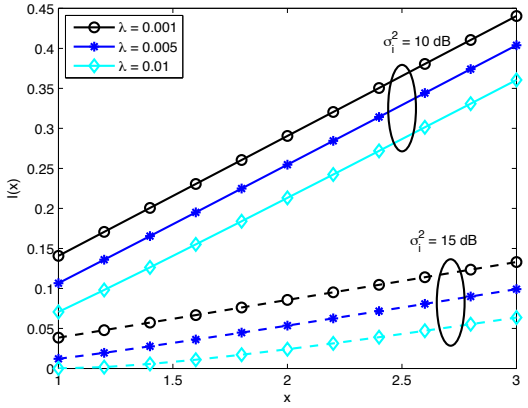

Fig. 3. The rate function is given for different values of the interference power and different values of the interferer density

VI. Conclusions

In this paper, we indicated how the energy consumption of a cognitive SAP is related to the detection performance. We demonstrated that the uncertainty of the interference environment results in the interference wall, beyond which no robust detection can be performed no matter how long the channel is observed. We derived an expression of the false alarm decay rate as a function of the sensing time, which evidences how the speed of convergence of $\mathbb{P}_{\text{fa}}$ is related to the interferer density and transmission power. In conclusion, the introduced concepts give insight into the robustness and the energy efficient operation of cognitive SAPs in heterogeneous networks.

References

[1] J. G. Andrews, H. Claussen, M. Dohler, S. Rangan, and M. C. Reed, "Femtocells: Past, present, and future," *IEEE J. Sel. Areas Commun.*, vol. 30, no. 3, pp. 497–508, Apr. 2012.

[2] H. Bogucka and A. Conti, "Degrees of freedom for energy savings in practical adaptive wireless systems," *IEEE Commun. Mag.*, vol. 49, no. 6, pp. 38–45, Jun. 2011.

[3] G. Gür and F. Alagöz, "Green wireless communications via cognitive dimension: An overview," *IEEE Netw.*, vol. 25, no. 2, pp. 50–56, Mar./Apr. 2011.

[4] Y. Chen, S. Zhang, S. Xu, and G. Li, "Fundamental trade-offs on green wireless networks," *IEEE Commun. Mag.*, vol. 49, no. 6, pp. 30–37, Jun. 2011.

[5] I. Guvenc, M. R. Jeong, I. Demirdogen, B. Kecicioglu, and F. Watanabe, "Range expansion and inter-cell interference coordination (ICIC) for picocell networks," in *Proc. IEEE Semiannual Veh. Technol. Conf.*, San Francisco, United States, Sep. 2011, pp. 1–6.

[6] W. C. Cheung, T. Q. S. Quek, and M. Kountouris, "Throughput optimization, spectrum allocation, and access control in two-tier femtocell networks," *IEEE J. Sel. Areas Commun.*, vol. 30, no. 3, pp. 561–574, Apr. 2012.

[7] I. Ashraf, F. Boccardi, and L. Ho, "Sleep mode techniques for small cell deployments," *IEEE Commun. Mag.*, vol. 49, no. 8, pp. 72–79, Aug. 2011.

[8] I. Haratcherev, M. Fiorito, and C. Balageas, "Low-power sleep mode and out-of-band wake-up for indoor access points," in *Proc. IEEE Global Telecomm. Conf.*, Honolulu, HA, Nov. 2009, pp. 1–6.

[9] L. Saker, S. E. Elayoubi, R. Combes, and T. Chahed, "Optimal control of wake up mechanisms of femtocells in heterogeneous networks," *IEEE J. Sel. Areas Commun.*, vol. 30, no. 3, pp. 664–672, Apr. 2012.

[10] T. Yucek and H. Arslan, "A survey of spectrum sensing algorithms for cognitive radio applications," *IEEE Commun. Surveys Tuts.*, vol. 11, no. 1, pp. 116–130, 2009.

[11] M. Chiani and A. Giorgetti, "Coexistence between UWB and narrowband wireless communication systems," *Proc. IEEE*, vol. 97, no. 2, pp. 231–254, Feb. 2009.

[12] I. Ashraf, L. Ho, and H. Claussen, "Improving energy efficiency of femtocell base stations via user activity detection," in *Proc. IEEE Wireless Commun. and Networking Conf.*, Sydney, Australia, Apr. 2010.

[13] M. S. Kay, *Fundamentals of Statistical Signal Processing: Detection Theory*, P. H. PTR, Ed., 1998.

[14] R. Tandra and A. Sahai, "SNR walls for signal detection," *IEEE J. Sel. Topics Signal Process.*, vol. 2, no. 1, pp. 4–17, Feb. 2008.

[15] A. Mariani, A. Giorgetti, and M. Chiani, "Effects of noise power estimation on energy detection for cognitive radio applications," *IEEE Trans. Commun.*, vol. 59, no. 12, pp. 3410–3420, Dec. 2011.

[16] D. Lopez-Perez, I. Guvenc, G. De La Roche, M. Kountouris, T. Q. S. Quek, and J. Zhang, "Enhanced intercell interference coordination challenges in heterogeneous networks," *IEEE Wireless Commun. Mag.*, vol. 18, no. 3, pp. 22–30, Jun. 2011.

[17] P. C. Pinto and M. Z. Win, "Communication in a Poisson field of interferers–Part I: Interference distribution and error probability," *IEEE Trans. Wireless Commun.*, vol. 9, no. 7, pp. 2176–2186, Jul. 2010.

[18] A. Rabbachin, T. Q. S. Quek, H. Shin, and M. Z. Win, "Cognitive network interference," *IEEE J. Sel. Areas Commun.*, vol. 29, no. 2, pp. 480–493, Feb. 2011.

[19] A. Rabbachin, A. Conti, and M. Z. Win, "Intentional network interference for denial of wireless eavesdropping," in *Proc. IEEE Global Telecomm. Conf.*, Houston, Texas, Dec. 2011, pp. 4268–4273.